Investigation of strain sensing effect in modified single-defect photonic crystal nanocavity

Bui Thanh Tung,[1] Dzung Viet Dao,[1] Taro Ikeda,[2] Yoshiaki Kanamori,[2] Kazuhiro Hane,[2] and Susumu Sugiyama[1,3,*]

[1]*Graduate school of Science and Engineering, Ritsumeikan University, Shiga, 525-8577, Japan*
[2]*Department of Nanomechanics, Graduate School of Engineering, Tohoku University, Sendai 980-8579, Japan*
[3]*Ritsumeikan-Global Innovation Research Organization, Ritsumeikan University, Shiga, 525-8577, Japan*
**sugiyama@se.ritsumei.ac.jp*

Abstract: This paper reports the theoretical and experimental investigations on the strain sensing effect of a two dimensions (2D) photonic crystal (PhC) nanocavity resonator. By using the finite element method (FEM) and finite difference time domain (FDTD) simulations, the strain sensitivity of a high quality factor PhC nanocavity was calculated. Linear relationships between the applied strain and the shift in the resonant wavelength of the cavity were obtained. A single-defect silicon (Si) PhC cavity was fabricated, and measurements of the strain sensitivity were performed. Good agreement between the experimental and simulation results was observed.

OCIS codes: (230.5298) Photonic crystals; (230.4685) Optical microelectromechanical devices; (000.4430) Numerical approximation and analysis.

References and links

1. T. F. Krauss, "Slow light in photonic crystal waveguides," J. Phys. D Appl. Phys. **40**(9), 2666–2670 (2007).
2. N. Skivesen, A. Têtu, M. Kristensen, J. Kjems, L. H. Frandsen, and P. I. Borel, "Photonic-crystal waveguide biosensor," Opt. Express **15**(6), 3169–3176 (2007).
3. W. Zhang, N. Ganesh, I. D. Block, and B. T. Cunningham, "High sensitivity photonic crystal biosensor incorporating nanorod structures for enhanced surface area," Sens. Actuators B Chem. **131**(1), 279–284 (2008).
4. Y. J. Lee, S. A. Pruzinsky, and P. V. Braun, "Glucose-sensitive inverse opal hydrogels: analysis of optical diffraction response," Langmuir **20**(8), 3096–3106 (2004).
5. T. Sünner, T. Stichel, S. Kwon, T. W. Schlereth, S. Hofling, M. Kamp, and A. Forchel, "Photonic crystal cavity based gas sensor," Appl. Phys. Lett. **92**(26), 261112 (2008).
6. Z. Xu, L. Cao, C. Gu, Q. He, and G. Jin, "Micro displacement sensor based on line-defect resonant cavity in photonic crystal," Opt. Express **14**(1), 298–305 (2006).
7. D. F. Dorfner, T. Hurlimann, T. Zabel, L. H. Frandsen, G. Abstreiter, and J. J. Finley, "Silicon photonic crystal nanostructures for refractive index sensing," Appl. Phys. Lett. **93**(18), 181103 (2008).
8. C. Lee and J. Thillaigovindan, "Optical nanomechanical sensor using a silicon photonic crystal cantilever embedded with a nanocavity resonator," Appl. Opt. **48**(10), 1797–1803 (2009).
9. B. Li and C. Lee, "Computational study of NEMS diaphragm sensor using triple nano-ring resonator," Procedia Eng. **5**, 1418–1421 (2010).
10. T. T. Mai, F. Hsiao, C. Lee, W. Xiang, C. Chen, and W. Choi, "Optimization and comparison of photonic crystal resonators for silicon microcantilever sensors," Sens. Actuators A Phys. **165**(1), 16–25 (2011).
11. T. Stomeo, M. Grande, A. Qualtieri, A. Passaseo, A. Salhi, M. De Vittorio, D. Biallo, A. D'orazio, M. De Sario, V. Marrocco, V. Petruzzelli, and F. Prudenzano, "Fabrication of force sensors based on two-dimensional photonic crystal technology," Microelectron. Eng. **84**(5-8), 1450–1453 (2007).
12. T. W. Lu and P. T. Lee, "Ultra-high sensitivity optical stress sensor based on double-layered photonic crystal microcavity," Opt. Express **17**(3), 1518–1526 (2009).
13. D. V. Dao, T. T. Bui, K. Nakamura, V. T. Dau, T. Yamada, K. Hata, and S. Sugiyama, "Towards highly sensitive strain sensing based on nanostructured materials," Adv. Nat. Sci: Nanosci. Nanotechnol. **1**(4), 045012 (2010).
14. B. Song, S. Noda, T. Asano, and Y. Akahane, "Ultra-high-Q photonic double-heterostructure nanocavity," Nat. Mater. **4**(3), 207–210 (2005).
15. S. Noda, A. Chutinan, and M. Imada, "Trapping and emission of photons by a single defect in a photonic bandgap structure," Nature **407**(6804), 608–610 (2000).

#141911 - $15.00 USD Received 28 Jan 2011; revised 9 Mar 2011; accepted 30 Mar 2011; published 21 Apr 2011

16. Y. Akahane, T. Asano, B. S. Song, and S. Noda, "High-Q photonic nanocavity in a two-dimensional photonic crystal," Nature **425**(6961), 944–947 (2003).
17. B. T. Tung, H. M. Nguyen, D. V. Dao, S. Rogge, H. Salemink, and S. Susumu, "Strain sensitivity of a modified single-defect photonic crystal nanocavity for mechanical sensing," in *Sensors, 2010 IEEE*, pp. 2585–2588, (Hawaii, Nov. 2010).
18. K. Okamoto, *Fundamentals of Optical Waveguides* (Academic Press, 2006).
19. M. Qiu, "Effective index method for heterostructure-slab-waveguide-based two-dimensional photonic crystals," Appl. Phys. Lett. **81**(7), 1163 (2002).
20. F. Shimokawa and H. Kuwano, "New high-power fast atom beam source," J. Vac. Sci. Technol. A **12**(5), 2739 (1994).
21. O. Svelto, *Principles of Lasers*, 4th ed. (Springer, 2009), Chap. 4.

1. Introduction

Photonic crystals (PhCs) are a periodic distribution of one material within a different host material having a different refractive index. PhCs show a variety of band dispersions and band gaps in which wave propagation is restricted for a certain range of wavelengths. By using different materials and adjusting geometrical parameters, the propagation of light can be modified in numerous ways and Si PhC-based devices have been widely used in light flow control applications, such as waveguides, photonic band gap structures, resonators, etc [1].

Recently, owing to various well-defined physical properties such as reflectance and transmittance and superior levels of sensitivity, which result in precise detection limits for optical measurements, PhC devices have been considered for use in sensing applications. PhC structures have been investigated for biosensing, chemical sensing, gas sensing and so on, owing to their sensitivity to small changes in the refractive index of the transmitted signal. These sensors detect the difference in the refractive index that corresponds to the molecule's immobilization in the PhC structures [2,3], ambient chemicals [4], or gas [5].

Mechanical sensing effects of PhC structures were also reported so far [6–13]. Xu et al. proposed a displacement sensor that uses the output light intensity as a sensing signal to detect movement [6]. Lee et al. reported on nanomechanical sensors using silicon photonic crystals that detect shifts in the resonant wavelength due to the application of force [7–10]. Stomeo et al. presented a force sensor utilized PhC optical filter structure by monitoring shift of resonant wavelength in transmission spectrum [11]. Lu and Lee reported the stress sensor based on double-layered photonic crystal cavity [12]. In these studies, the influence of the orientation of the generated stress/strain on the sensitivity measurements was not taken into account. Furthermore, the experimental results were not reported.

In this paper, theoretical and experimental investigations of the mechanical stress/strain sensitivity of a 2D photonic crystal (PhC) nanocavity resonator are discussed. By using the finite element method (FEM) and finite difference time domain (FDTD) simulations, the change in the resonant wavelength of a high Q-factor cavity due to the application of stress/strain was analyzed. The cavity was fabricated on a silicon-on-insulator (SOI) wafer for experimental verification. A simple and effective cantilever structure was used to apply mechanical stress/strain to the PhC structure for the sensing effect measurements.

2. Strain sensing principle and PhC device for strain sensing

2.1 Strain sensing principle

A schematic of a 2D Si PhC structure is shown in Fig. 1. It consists of an air-hole lattice with a particular diameter and pitch. When a mechanical stress/strain is applied to the PhC structure, the geometry of the air-hole lattice will be changed, leading to a change in its optical properties. These strain-induced changes in optical properties can potentially be applied to stress/strain sensing applications.

#141911 - $15.00 USD Received 28 Jan 2011; revised 9 Mar 2011; accepted 30 Mar 2011; published 21 Apr 2011

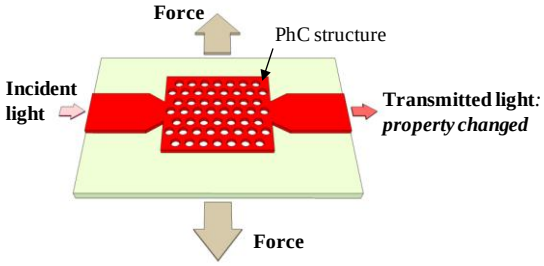

Fig. 1. Schematic of 2D PhC structure under stress/strain.

In order to evaluate this effect, the change in the optical signal when a mechanical stress/strain is applied needs to be evaluated. One of the implementable ways is to detect the change in the light transmitted through the PhC device, i.e., the change in intensity at a specific wavelength or the shift in the wavelength of the peak intensity. Here, detection of the shift in the wavelength was chosen as the measurement method owing to its lower sensitivity to noise (which usually affects the signal level) than the intensity detection method. Cavity structure, with ability to strongly confine light so that only certain wavelengths, called resonant wavelengths, inside the band gap of the PhC structure can be supported to pass through, is a good candidate for strain sensing application. In this study, the shift in the resonant wavelength induced by the strain was investigated both theoretically and experimentally. High resolution mechanical strain sensing is expected owing to the high SNR of the optical measurement technique.

2.2 Design of PhC cavity

Among the PhC structures proposed (in one, two and three dimensions), 2D PhC slab cavity have been the subject of intense research activity. It can be fabricated from a single thin silicon layer by micromachining technology. PhC cavity structures with the ability to strongly confine light are very important for a variety of scientific and engineering applications. Over the past few years, many studies have focused on optimizing the cavity geometry and the mode supported by it [14–16]. In our work, these structures were used to study the strain sensing effect. A theoretical analysis of the strain sensing capability of a single defect in ΓM direction PhC cavity has been previously reported by the authors [17]. In this paper, the ΓK direction PhC cavity is considered. Both theoretical and experimental investigations of the sensing effect in this cavity will be discussed.

In this work, a cavity structure was created by removing three air holes along the ΓK direction in a 2D triangular lattice PhC slab, as shown in Fig. 2. The radius of the air holes was $r = 0.333a$ (where $a = 450$ nm is the lattice constant). The in-plane confinement of light was guaranteed by the PhC structure, and the out-of-plane confinement was due to the total internal reflection at the Si–SiO_2 and Si–air interface. The Q-factor of the cavity was enhanced by tuning the cavity length d, which was achieved by shifting the outer holes, thus introducing dislocations in the lattice [16]. Simulation results show the highest Q-factor was obtained when the two outer holes were shifted by $0.15a$ from the original lattice positions. Both ends of the PhC resonator were connected to a ridged waveguide system ending in a cleaved facet. These facets were used for coupling light to the device.

The cavity was modeled using FDTD software. An equivalent 2D structure was obtained by using the effective refractive index approximation method [18]. This method reduces the calculation time yet agrees well with a full 3D FDTD approach [19]. The effective refractive index of air/260nm-Si/2μm-SiO_2 was computed to be 2.98 at a wavelength of 1.5 μm. The SiO_2 layer in our study is not removed and is utilized to transmit the stress/strain from substrate to PhC layer.

#141911 - $15.00 USD Received 28 Jan 2011; revised 9 Mar 2011; accepted 30 Mar 2011; published 21 Apr 2011

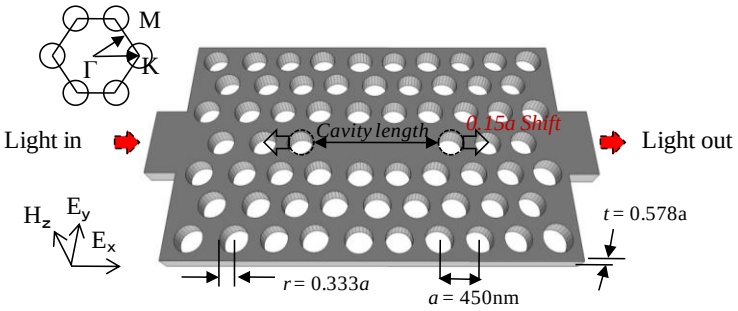

Fig. 2. Configuration of photonic crystal cavity to investigate strain sensing effect where r/a = 0.333 and lattice constant a = 0.45 nm. The red arrows indicate the launching direction of light used for exciting the resonator.

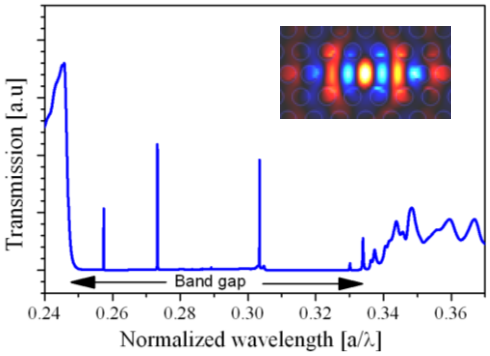

Fig. 3. Transmission spectrum of resonant modes showing cavity peaks at 0.2573(a/λ), 0.2733(a/λ), and 0.3037(a/λ). The inset shows the intensity profile of a degenerate mode obtained using FDTD simulations.

The analysis performed in this work was mainly focused on the TE polarization light. Figure 3 shows the output transmission spectrum in the free stress/strain status. The results show a resonant mode at normalized wavelengths of 0.2573 (a/λ), 0.2733 (a/λ), and 0.3037 (a/λ), which correspond to resonant wavelengths of 1748.9 nm, 1646.5 nm, and 1481.7 nm, respectively, in the band gap range between 0.248 (a/λ) and 0.335 (a/λ). The shifts in these resonant wavelengths were recorded during the application of mechanical strain.

3. Theoretical analysis of strain sensitivity

First, changes in the geometry of the PhC when subject to stress/strain were analyzed using FEM. Then, these changes in geometry, such as the hole's position and shape, were used as input parameters for the FDTD simulation in order to obtain the transmission spectrum.

The sensing effects were evaluated for two different cases: longitudinal strain, i.e., strain applied parallel to the direction of light propagation; and transverse strain, i.e., strain applied perpendicular to the propagation of light.

#141911 - $15.00 USD Received 28 Jan 2011; revised 9 Mar 2011; accepted 30 Mar 2011; published 21 Apr 2011

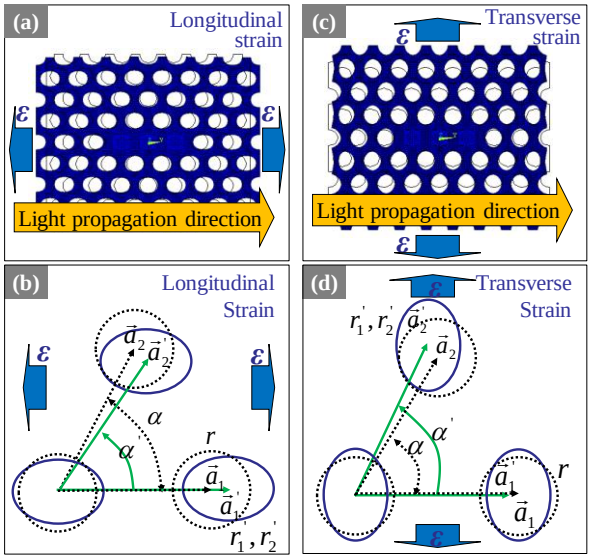

Fig. 4. Deformation of PhC structure under applied strain. In (a) and (c), dashed and solid shapes show the initial and under-strain shape of the PhC, respectively. Changes in the PhC lattice geometry are shown schematically in (b) and (d).

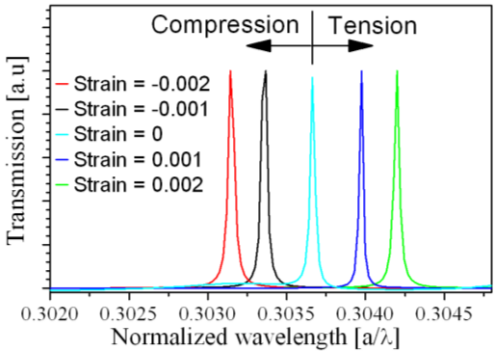

Fig. 5. Transmission spectrum showing resonant wavelength vs. different strain values.

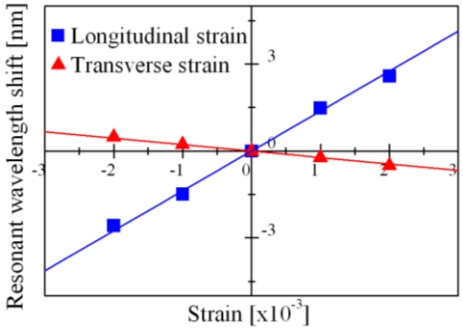

Fig. 6. Resonant wavelength shift vs. strain.

Figure 4 shows the simulation results of the PhC structure obtained using ANSYS™ under elastic strains that correspond to the longitudinal and transverse directions. In this simulation, the Young's modulus and Poisson's ratio of 169 GPa and 0.28 were used for Si, respectively. This clearly shows that holes were distorted and relocated. The new positions and shapes of the air holes were calculated as shown schematically in Figs. 4(b), 4(d). These were used as input parameters for the FDTD simulation.

The FDTD simulation results are shown in Figs. 5 and 6. Both tensile and compressive strains were considered in our study. Figure 5 shows the shift in the resonant wavelength of the 0.3037 (a/λ) peak, resulting from the longitudinal strain. It can be seen that under longitudinal tensile strain, the resonant wavelength tended to shift to a longer wavelength, whereas it tended to shift to a shorter wavelength under transverse tensile strain. The wavelength shifts were calculated to be 1.48 pm/με and 0.25 pm/με for longitudinal and transverse strains, respectively. The relationship between applied stress/strain and resonant shift is linear in interested stress/strain range. Figure 6 shows the simulation results for the shift in the resonant

#141911 - $15.00 USD Received 28 Jan 2011; revised 9 Mar 2011; accepted 30 Mar 2011; published 21 Apr 2011

wavelength due to longitudinal and transverse strains. The difference in the shifts in resonant wavelength because of longitudinal and transverse strains highlights the anisotropic property of the strain sensing effect of the PhC cavity.

4. Fabrication of silicon PhC device

The test structure was fabricated using micro-machining, as shown in Fig. 7. The starting wafer (Fig. 7(a)) was intrinsic SOI, where the thickness of the Si device layer, SiO_2 layer, and the total wafer thickness were 260 nm, 2 μm, and 650 μm, respectively. Firstly, electron beam lithography (EBL) and developmental processes were performed to pattern the PhC and the waveguide structures (Fig. 7(b)). A fast atom beam (FAB) etching process [20] was then used to create PhC nanostructures (Fig. 7(c)). Finally, a cleaving process was used to separate the chip and form the clean and flat facets, which were used for the in- and out-coupling of the light entering into and exiting out of the PhC, respectively, via integrated Si waveguides (Fig. 7(d)).

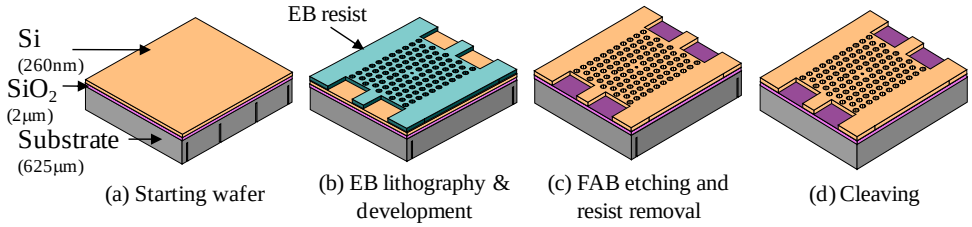

Fig. 7. Fabrication process.

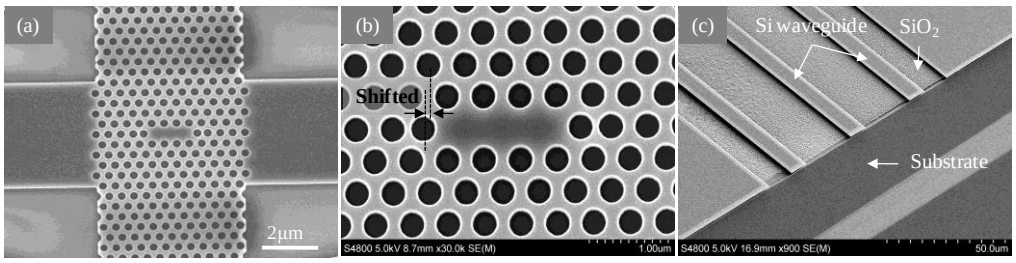

Fig. 8. SEM images of photonic crystal structure after fabrication. (a) Top view, (b) enlarged image of defective area, (c) in- and out-coupling facet after cleaving.

Scanning electron microscopy (SEM) pictures of the PhC structure after fabrication are shown in Fig. 8. In Fig. 8(a), the top view of the device, including the cavity and feeding waveguide is shown. A detailed view of the defective area is shown in Fig. 8(b), and Fig. 8(c) shows a good facet for coupling purposes.

5. Measurements and discussion

5.1 Measurement setup

The characteristics of the fabricated PhC cavity were evaluated using the transmission measurement system, shown schematically in Fig. 9(a). Polarized tunable light (with a wavelength of λ = 1460–1580 nm) from a diode laser was coupled to a lensed fiber with a focal length of 25 μm. Only TE-like polarized light was coupled to the PhC structure. The light transmitted through the PhC structure was coupled to another lensed fiber at the out-coupling facet and then guided onto the photo detector (Agilent 8164A). An infrared camera was used to support the coupling of light between the sample facets and the lensed fiber.

#141911 - $15.00 USD Received 28 Jan 2011; revised 9 Mar 2011; accepted 30 Mar 2011; published 21 Apr 2011

Strain was generated with a cantilever system, as shown in Fig. 9(b). The test sample, which was cleaving as a cantilever with dimensions of 15000 μm × 2500 μm × 625 μm (length × width × thickness), was mounted on a fixed base using epoxy. The PhC cavity was placed near the fixed end of the cantilever in order to realize large strain. The free end of the cantilever was hung by standard weights. The strain generated in the PhC structure was calculated using the equation:

$$\varepsilon = \frac{6mg(l-x)}{Ebh^2}. \tag{1}$$

where m is the mass of the weight; g is gravity; E is the Young's modulus of Si; x is the distance from the cavity position to the fixed edge of the cantilever; and l, b, and h are the length, width, and thickness of the cantilever, respectively.

Weights of 100 g and 150 g were consecutively suspended from the tip of the cantilever to create longitudinal strains of 295 × 10^{-6}, and 433 × 10^{-6}, respectively. The transmission spectra of the PhC structure at these different applications of strain were measured to determine the strain sensing effect of the PhC cavity structure.

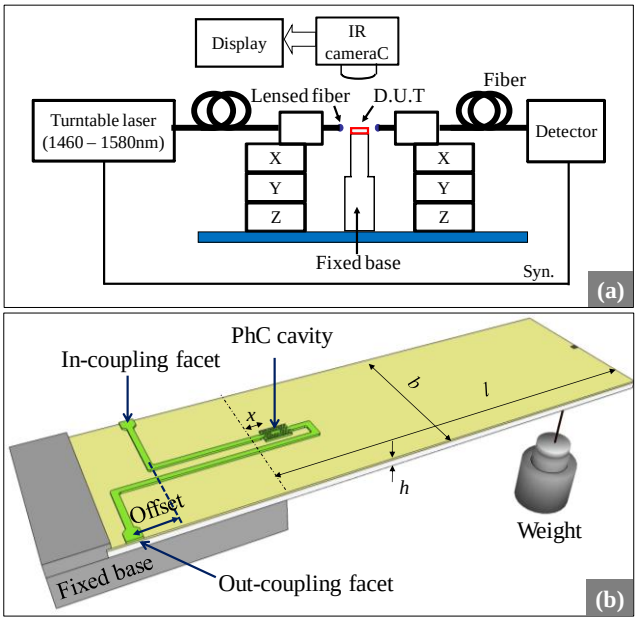

Fig. 9. Schematic of experimental setup. (a) Transmission spectral measurement system and (b) mechanical strain loading model.

In the design, the in- and out-coupling facets were located in the fixed part of the cantilever so that the facets did not move during the application of force; therefore, re-alignment problems between the fiber lens and the facets were avoided. The out-coupling facet was also offset from the in-coupling facet so as to prevent direct propagation of the incident ray to the lensed fibers at the output.

5.2 Measurement results and discussion

The transmission spectrum of the cavity is shown in Fig. 10. The red line represents the curve of best fit. Although the interface between the waveguide and the PhC cavity could have been optimized for more efficient coupling, a resonant peak at a wavelength of 1487.55 nm was obtained with a Q-factor of 4500. The small difference in the resonant wavelength between the

#141911 - $15.00 USD Received 28 Jan 2011; revised 9 Mar 2011; accepted 30 Mar 2011; published 21 Apr 2011

experiment and the simulation was attributed to the differences in the actual hole geometry between design and fabrication.

Figure 11 shows resonant peaks corresponding to applied strains of 0, 295 × 10^{-6}, and 433 × 10^{-6}, respectively. It can clearly be seen that when a tensile stress was applied to the PhC cavity, the resonant peak shifted to a longer wavelength. This agrees well with the simulation results. The shift was measured to be 0.95 pm/10^{-6} strain.

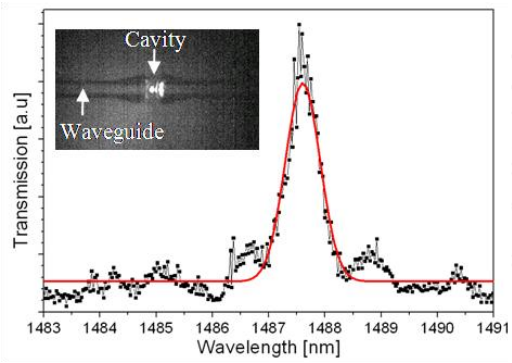

Fig. 10. Transmission spectrum of fabricated cavity. The inset shows the near field image observed using an infrared camera from the top of the cavity.

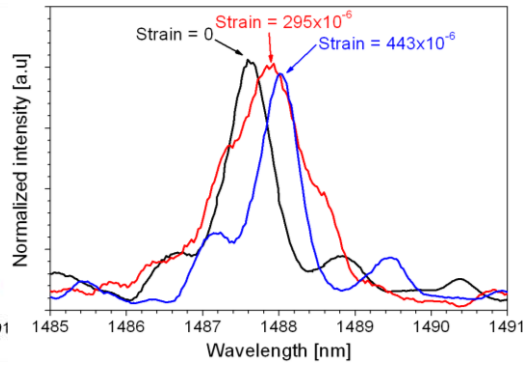

Fig. 11. Shift in resonant wavelength of cavity due to application of strain.

The gauge factor of the PhC cavity was defined as the change in the resonant wavelength due to the application of strain, as given in Eq. (2):

$$G = \frac{d\lambda}{\lambda}. \qquad (2)$$

On the basis of these measurement results, the gauge factor was calculated to be 0.64. Owing to the advantages of the optical measurement technique, which provides a minimum detectability of 0.008 pm for a current commercial optical spectrum analyzer (e.g., Agilent-83453B-HRS), the theoretical minimum detectable strain for this PhC cavity was up to 8.5 × 10^{-9} (8.5 nε).

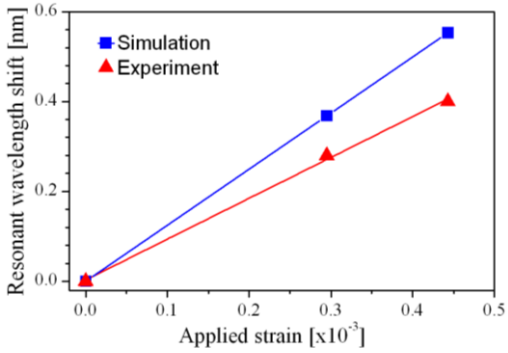

Fig. 12. Strain induced shifts in resonant wavelength.

Figure 12 shows the linear relationship between the applied strain and the shifts of resonant wavelength. This behavior is analogous to that of transmission peak shift of a Fabry-Perot

#141911 - $15.00 USD Received 28 Jan 2011; revised 9 Mar 2011; accepted 30 Mar 2011; published 21 Apr 2011

cavity when its cavity length changes [21]. With this linear relationship, it is possible to detect strain based on measurement of resonant wavelength shift.

The measured shifts in the wavelength and the calculated gauge factor were slightly smaller than simulation values (Fig. 12). The reason for this could have been a mismatch between the calculated and actual strain and imperfections in the fabricated structure. The mismatch between the calculated and actual strains may be caused by misalignment between the sample and the base after mounted. This effect could be eliminated by integrating a reference strain gauge, i.e., a piezoresistive resistor, to measure the actual strain. Imperfections in the cavity's sharpness could be due to the surface roughness of the Si slab, surface roughness of the inner walls of the air holes, or variations in the radii of the air-holes as well as their sharpness. Under an applied strain, these imperfections could have a significant effect on the cavity's peak position. This issue could be diminished by optimizing the fabrication process.

Another reason courses the mismatch between the simulated and measured results could be the influence of strain to material's refractive index, which was not included in the simulation. Strain makes the total refractive index changes due to the two effects: change of geometry of the holes lattice, and change of refractive index of the material [17]. However, because the PhC structure consists of periodically-distributed air holes on Si slab, the stress/strains are distributed non-uniformly in the Si slab, and therefore, the refractive index of material is also distributed non-uniformly in the material. This makes the simulation becomes difficult and not yet be solved completely.

6. Conclusion

The strain sensitivity of a Si PhC cavity resonator was investigated by performing simulations and actual measurements.

The strain-induced optical properties of the PhC were studied by using a combination of FEM and FDTD simulations. The results highlight the anisotropic property of the strain sensing effect of the PhC cavity. Further, a linear relationship between the applied strain and the shift in the resonant wavelength was obtained.

A fabrication process, which consisted of direct EB lithography, FAB etching, and cleaving, was employed to realize the test sample. Different strains were applied to the fabricated cavity structure via a simple and effective cantilever system. Experimental results showed strain-induced shifts in the resonant wavelength of a single-defect PhC nanocavity when a longitudinal strain was applied. Measurement of the shift in the resonant wavelength due to transversal strain remains as future work.

The initial obtained results from this study call for further research to apply this potential strain sensing effects of PhC cavities to applications such as PhC-based mechanical sensing devices.

Acknowledgments

This study was partly supported by the Ministry of Education, Culture, Sports, Science and Technology of Japan under the Grant-in-Aid for Young Scientists (No.21710141-0001).

#141911 - $15.00 USD Received 28 Jan 2011; revised 9 Mar 2011; accepted 30 Mar 2011; published 21 Apr 2011